Title

Machine Learning Identifies a Rat Model of Parkinson's Disease via Sleep-Wake Electroencephalogram

Authors

Lu, Jun
Sorooshyari, Siamak K

Publication Date

2023-02-01

DOI

10.1016/j.neuroscience.2022.11.035

Peer reviewed

NEUROSCIENCE
RESEARCH ARTICLE

J. Lu, S. K. Sorooshyari / Neuroscience 510 (2023) 1–8

Machine Learning Identifies a Rat Model of Parkinson's Disease via Sleep-Wake Electroencephalogram

Jun Lu [a]* **and Siamak K. Sorooshyari** [b]*

[a] *Stroke Center, Department of Neurology, 1st Hospital of Jilin University, Changchun 120021, China*

[b] *Department of Integrative Biology, University of California, Berkeley, Berkeley, CA 94720, USA*

Abstract—Alpha-synuclein induced degeneration of the midbrain substantia nigra pars compact (SNc) dopaminergic neurons causes Parkinson's disease (PD). Rodent studies demonstrate that nigrostriatal dopamine stimulates pallidal neurons which, via the topographical pallidocortical pathway, regulate cortical activity and functions. We hypothesize that nigrostriatal dopamine acting at the basal ganglia regulates cortical activity in sleep and wake state, and its depletion systemically alters electroencephalogram (EEG) across frequencies during sleep-wake state. Compared to control rats, 6-hydroxydopamine induced selective SNc lesions increased overall EEG power (positive synchronization) across 0.5–60 Hz during wake, NREM (non-rapid eye movement) sleep, and REM sleep. Application of machine learning (ML) to seven EEG features computed at a single or combined spectral bands during sleep-wake differentiated SNc lesions from controls at high accuracy. ML algorithms construct a model based on empirical data to make predictions on subsequent data. The accuracy of the predictive results indicate that nigrostriatal dopamine depletion increases global EEG spectral synchronization in wake, NREM sleep, and REM sleep. The EEG changes can be exploited by ML to identify SNc lesions at a high accuracy.

Key words: Parkinson's disease, machine learning, electroencephalogram, sleep-wake cycle, dopamine, biomarker.

INTRODUCTION

Alpha-synuclein induced degeneration of pigmented dopaminergic neurons in the midbrain substantia nigra pars compact (SNc) is responsible for hallmark motor and non-motor symptoms of Parkinson's disease (PD). Prior animal studies have established the neural circuitry of SNc dopamine control of the cerebral cortex. Specifically, nigrostriatal dopamine acting on D2 receptors at the presynaptic sites of striatopallidal axons activates the external globus pallidus (GPe) GABAergic neurons that, via pallidocortical projections, regulate cortical activity and functions (Chen et al., 2015; Qiu et al., 2016b, 2019; Guo et al., 2017). Furthermore, selective 6-hydroxydopamine lesions of SNc dopaminergic neurons have been found to increase cortical activity as shown by c-Fos expression and increased total wakefulness in rats (Qiu et al., 2014, 2016b, 2019). These observations and the neural circuitry of SNc dopamine control of the cerebral cortex suggest that nigrostriatal dopamine loss (SNc lesion) causes extensive elevation in global cortical activity of electroencephalogram (EEG). Although unusually high beta EEG power has been reported in human and rat PD models (Sharott et al., 2005; Deffains and Bergman, 2019), it has not been determined if EEG changes occur at other frequencies, whether the EEG changes persist during wake and sleep states, and if machine learning (ML) can distinguish EEG changes in sleep-wake caused by the SNc lesions. We made selective ablations to SNc dopamine neurons and systemically examined 0.5–60 Hz changes in EEG during wake, NREM sleep, and REM sleep. Compared to human PD that has lesions far beyond the nigral dopaminergic neurons, the rat PD model of 6-hydroxydopamine lesions is confined to SNc dopaminergic neurons, thus a rat PD model is appropriate for analyzing the changes of SNc lesions. The ML analysis is supervised since our algorithm is provided with data, the outputs that the data should produce, and then the algorithm is asked to classify unencountered data based on what it has learned. The ML techniques' accuracy on unencountered data will dictate the efficacy of the analysis as well as whether the data contains categorical structure. Our results show that SNc lesions increased 0.5–60 Hz EEG power, and that the computed features used to train a support vector

*Corresponding authors.
E-mail addresses: lujun@jlu.edu.cn (J. Lu), siamak_sorooshyari@berkeley.edu (S. K. Sorooshyari).
Abbreviations: EEG, Electroencephalogram; GPe, external globus pallidus; ML, machine learning; NREM, Non-rapid eye movement; PD, Parkinson's disease; SNc, substantia nigra pars compact; VTA, ventral tegmental area.

https://doi.org/10.1016/j.neuroscience.2022.11.035
0306-4522/

machine (SVM) are able to distinguish the lesioned animals from controls at a high accuracy.

METHODS

6-hydroxydopamine (6-OHDA) lesions of SNc dopamine neurons

The SNc lesioned and control Sprague-Dawley rats (300 g male, Harlan) used in this study have been examined for sleep-wake changes where 6% 6-hydroxydopamine (6-OHDA) injections in the ventral pallidum bilaterally ablated more than 80% of the SNc dopamine neurons and significantly reduced sleep amounts with sleep-wake fragmentation. The animals were 8 weeks old (w.o.). The Institutional Animal Care and Use Committee of Beth Israel Deaconess Medical Center approved all protocols. The methods for 6-OHDA injection, SNc lesion, EEG/EMG/video recording, and sleep-wake changes were reported previously (Qiu et al., 2016b). Breifly,100 nl 6% 6-OHDA (Sigma) injected into the ventral pallidal region was taken up by the dopaminergic terminals and killed dopaminergic neurons in the SNc and their dorsal striatum terminals yet spared the ventral tegmental area (VTA) and ventral striatum. This method effectively ablated about 80–90% of the SNc. EEG/EMG signals were amplified (AM systems, USA), digitized and recorded (256 Hz sampling) using vital recorder software (CED ltd. Cambridge, UK) and sleep-wake analyses were done by SleepSign. Wake (12 s per episode) was identified by online low EEG amplitude and high EMG and posture on synchronized video; NREM sleep (12 s per episode) was identified by high EEG amplitude and low EMG and sleep posture. REM sleep (12 s per episode) was identified by extremely high ratio of theta power/delta power and very low EMG and sleep posture. However, spectral analysis was not performed on the EEG. In the present study, extracted data from EEG of nine SNc lesioned animals and nine sham controls were used for statistical analyses and as inputs to a machine learning (ML) algorithm to determine whether the SNc lesioned animals could be distinguished from the controls.

Feature analysis. After 2-week recovery from the surgery of bilateral 6-hydroxydopamine injection at the ventral pallidal region (N = 9) or sham surgery (N = 9), rats were connected to EEG/EMG recording for 1 day of acclimation and EEG/EMG/video was then recorded for 24 h. The EEG/EMG was collected at a sampling rate of 256 Hz. The 0-Hz measurement was discarded and artifact removal was performed by deleting all samples that exceed a threshold set to five times the mean value of the measured power at 0.5 Hz. The power levels at the frequencies were consolidated into seven bands: *delta (0.5–4 Hz), theta (4.5–8 Hz), alpha (8.5–12 Hz), beta (12.5–20 Hz), high-beta (20.5–30 Hz), low-gamma (30.5–40 Hz),* and *high-gamma (40.5–60 Hz).* For each sample, the mean power was computed by averaging across the frequencies that comprised the spectral bands – this resulted in seven power levels per time instant. While the 24-h recordings were collected at a 256 Hz sampling rate, each mean power value was calculated by averaging over 12 s. A second level of artifact removal was applied by discarding samples with a value in any of the seven frequency bands that exceeded 10 μV^2/Hz. This was done while being cognizant of the inverse power law of the electrophysiological power spectral density (Buzsaki and Draguhn, 2004). Specifically, the high threshold was selected to remove rare events (i.e. artifacts) and not affect the underlying relation between the power levels of each band. The EEG power of each animal across the seven frequency bands were separated based on whether they occurred during wake, REM, or NREM. Each animal's per-state recording was then input to in-house MATLAB scripts to compute the features that were used as inputs to the ML analysis.

Computed features. Five statistical features were attained for each of the seven spectral bands in a recording by computing the *mean, variance, median, minimum,* and *maximum* of the EEG signal. This was performed after the EEG signal was filtered in each of the bands. We also computed the number of deviations (ND) by Z-scoring the signal and declaring a deviation-low when the signal was less than -2σ and a deviation-high when the signal exceeded 2σ. The number of low and high deviations were normalized by the number of samples in the recording with the results being referred to as ND-low and ND-high, respectively. The deviation features are a measure of the burstiness or paroxysmal nature of the EEG signal. It should be noted that the features have been selected to be simple, reflective of the temporal properties of the EEG signal, while not being redundant of one another – i.e. none of the features can be faithfully reproduced from the remainder of the features. Thus, five statistical and two deviation-based features were collected for each of the seven frequency bands of an animal during REM sleep, NREM sleep, and wakefulness.

Statistical analysis. A Kolmogorov-Smirnov (KS) test was performed to assess the possibility of features being sufficiently different among the EEG recordings from the two groups of animals. The p-value associated with each feature rejecting the null hypothesis of being different among the SNc lesioned and control cohorts is reported via the same technique. In the specific case of the increase in a paroxysmal feature in the high gamma band during REM sleep, a KS test was used to assess statistical significance (p-value < 0.05) between SNc lesioned animals and controls. The result was conveyed via a box-and-whisker plot with the lower and upper quartiles as the edges of the shaded box and the whiskers corresponding to the minimum and maximum values. A Shapiro–Wilk test was applied to the temporal recordings across the seven frequency bands of all animals (N = 18, SNc lesioned and controls) for each of the three sleep/wake states to assess the normality of the signals. Nearly all (374/378) outcomes rejected the null hypothesis (p-value < 0.05) of the EEG signal being Gaussian.

Machine learning analysis. The features computed across the different EEG frequency bands from each sleep-wake state of an animal were arranged in a vector and used either as training or test data in the ML analysis. The ML technique used was a support vector machine (SVM) with a linear kernel and a binary classifier. The ML and cross-validation techniques were implemented in R via the e1071 and kernlab packages. To use a balanced training set, computed EEG features of eight control and eight PD animals were randomly selected and used to train the SVM. Subsequently, the remaining SNc-lesioned recording and control recording were considered as the two test data points. The trained machine's classification decisions were compared to the ground-truth labels associated with the two left-out data points. This process was iterated 1000 times to attain a mean classification accuracy rate. A schematic of the pipeline is shown in Fig. 1 with the sets A and B corresponding to the recordings from control and SNc lesioned animals. In assessing the results, we refer to an accuracy rate of 0.65 as being desirable since it is approximately-one-sigma greater than the chance value of 0.5 (binary classification). For comparison, the ML pipeline was repeated with an L1 regularized logistic regression (L1-LR) used in place of the SVM with the aim of providing a solution that potentially improves predictive capability in situations where SVM may be overfitting. The L1-LR was implemented via the glmnet package in R with a binomial family and five folds.

RESULTS

To investigate whether and how SNc dopamine depletion alters cortical activity, we examined the effect of SNc lesions on the EEG and whether ML was able to distinguish SNc-lesioned animals from the controls. Compared to controls, 6-OHDA lesions of bilateral SNc (nigrostriatal dopamine depletion) produced an increase

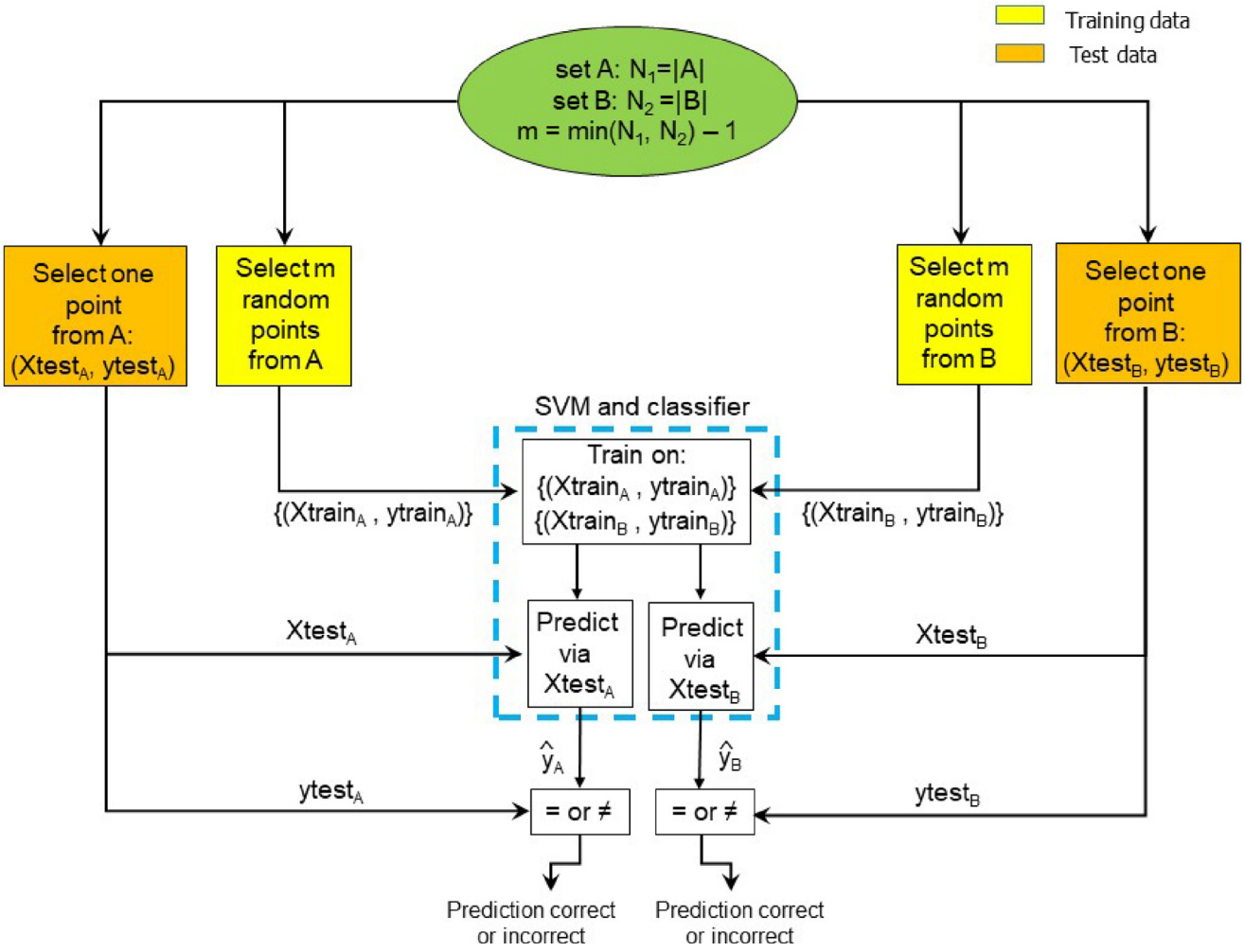

Fig. 1. The machine learning (ML) pipeline used to predict whether features computed from EEG recordings can be used to distinguish lesioned rats from controls. The sets A and B correspond to features computed from the EEG recordings of control and SNc lesioned rats. The notation |.| refers to the number of elements in the set (i.e. cardinality), while "^" denotes the predicted value of a label from the test data. The above workflow was iterated at 1000 independent realizations to arrive at a classification accuracy rate. Each iteration encompassed an SVM trained on features prior to being presented with test data in the form of a left-out sample from each of the two categories. A correct prediction corresponds to $\hat{y} = y_{test}$ for a left-out sample from set A or B. The accuracy rate was attained by calculating the fraction of times the labels of the left-out samples were correctly predicted.

in nearly all (104/105) statistical features across the EEG spectra with significance ($p < 0.05$) or near significance ($0.05 < p < 0.1$) as seen in Fig. 2(**A**) and Table 1. The consistent increase in the statistical features indicated elevated EEG power across spectra, i.e. increased positive EEG synchronization in the 0.5–60.0 Hz range. The total number of EEG features with statistical significance among SNc lesion and control were 18 in wake, 11 in NREM sleep, and 10 in REM sleep. A significance level of $0.05 < p < 0.1$ was seen in 14 of the features during wake, 21 features in NREM sleep, and 20 features in REM sleep (Fig. 2(**A**)). Although EEG features were increased across spectral bands, certain bands showed particularly robust increases in two or all three sleep-wake states. For instance, low gamma oscillation was noted during wake and NREM sleep, theta oscillation in wake and REM sleep, and delta oscillation in REM and NREM sleep. Beta

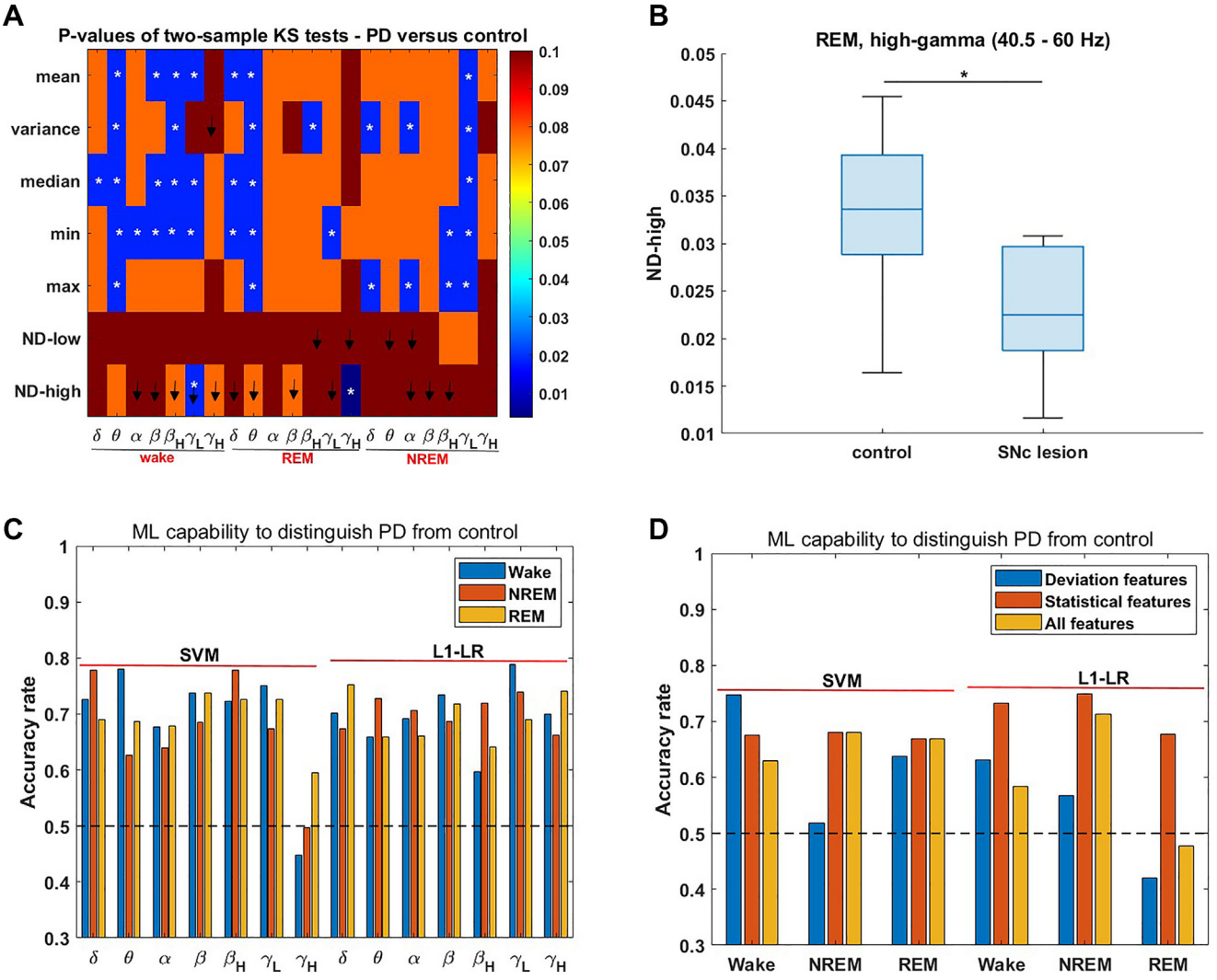

Fig. 2. Statistical and ML analysis on SNc-lesion induced EEG changes during wake, REM sleep, and NREM sleep. A Kolmogorov-Smirnov (KS) test was applied to assess seven features (y-axis) from EEG signals being sufficiently different between the control (N = 9, age = 8 w.o.) and SNc lesioned (N = 9, age = 8 w.o.) animals. Five statistical and two deviation-based features from the delta (δ), theta (θ), alpha (α), beta (β), high beta (β_H), low gamma (γ_L), and high gamma (γ_H) (x-axis) EEG were evaluated during wake, NREM sleep, and REM sleep in the two groups. SNc lesions altered statistical and deviation-based features via mostly increasing the feature values with a few reductions (indicated by the down arrows). Of the deviation features across all spectra, only the low gamma in wake and high gamma in REM were statistically significant ($p < 0.05$ – indicated by white stars) between the two animal groups. ML analysis was performed on EEG features to distinguish between the control and SNc-lesioned animals during three sleep/wake states (**A**). It is noted that in the high gamma band (40.5–60 Hz) the increase in the ND-high feature during REM sleep for SNc lesioned animals in comparison to controls was statistically significant (KS test, $p < 0.05$). The lower and upper quartiles appear as the edges of the shaded box while the whiskers have endpoints that correspond to the minimum and maximum values (**B**). Using an SVM, the ML pipeline differentiated EEG features in sleep-wake states between PD and control animals at an accuracy rate greater than 0.65 at each spectral band except for high gamma. The black, dashed line indicates the chance predictive value of 0.5 for binary classification. Similar results were noted with the L1-LR technique although the predictive capability was degraded in the high beta rather than the high gamma band (**C**). With respect to the different groups of features, barring the deviation features during NREM sleep, when provided with the statistical, deviation, or all features across the spectrum of considered frequencies, the SVM distinguished SNc lesioned animals from controls at high accuracy during wake, REM sleep, and NREM sleep. Similar results were noted with L1-LR except the predictive capability was poor during REM sleep when considering all features or only the deviation features (**D**).

Table 1. The number of statistically significant EEG features between SNc lesioned and control rats in sleep-wake states

EEG spectral band	Wake	REM	NREM
Delta (0.5–4 Hz)	1 (1,0)	3 (3,0)	2 (2,0)
Theta (4.5–8 Hz)	5 (5,0)	5 (5,0)	0 (0,0)
Alpha (8.5–12 Hz)	1 (1,0)	0 (0,0)	2 (2,0)
Beta (12.5–20 Hz)	3 (3,0)	0 (0,0)	0 (0,0)
High-beta (20.5–30 Hz)	4 (4,0)	1 (1,0)	2 (2,0)
Low-gamma (30.5–40 Hz)	4 (3,1)	1 (1,0)	5 (5,0)
High-gamma (40.5–60 Hz)	0 (0,0)	1 (0,1)	0 (0,0)

The table entry a(b,c) denotes the total number of statistically significant features (a) as well as the number of significant statistical (b) and deviation (c) features. A threshold of $p = 0.05$ was considered significant for the Kolmogorov-Smirnov test results in Fig. 2. Across the wake, NREM sleep, and REM sleep states, 38 statistical features and 2 deviation features (low gamma in wake, high gamma in REM) were significant.

oscillation as well as delta oscillation were noted in all three states (Fig. 2(**A**), Table 1).

We further quantified the degree of global EEG spectral synchronization across a frequency band by taking the ratio of the mean power between the depleted and control case. This is referred to as the rise in synchronization and shown in Table 2 for the sleep-wake states. We noted that the rise in synchronization was significant across all of the frequency bands in NREM sleep and nearly all bands during wake and REM sleep. The greatest rise in synchronization was noted at the delta and theta frequency bands during wake as well as REM sleep. During NREM sleep the highest value of this metric occurred in high beta. While in all three states the least degree of synchronization by the SNc lesions was seen at the high gamma band, the result was not significant during wake and REM sleep. It is interesting that the high gamma is the only frequency band that showed low but not significant increases in wake and REM sleep. REM sleep, NREM sleep and wake showed a general trend of increased rise in synchronization at the lower frequencies with the effect lessening at the higher frequencies.

Table 2. The rise in a synchronization metric reflects the increase in mean power at a frequency band as the measure of global EEG spectral synchronization

Sleep-wake state	Frequency band	Rise in synchronization
Wake	Delta *	7.02
Wake	Theta *	6.28
Wake	Alpha *	5.54
Wake	Beta *	5.28
Wake	High beta *	5.93
Wake	Low gamma *	4.85
Wake	High gamma	2
NREM	Delta *	5.99
NREM	Theta *	5.41
NREM	Alpha *	5.51
NREM	Beta *	5.3
NREM	High beta *	6.39
NREM	Low gamma *	6.19
NREM	High gamma *	3.5
REM	Delta *	6.25
REM	Theta *	7.04
REM	Alpha *	5.25
REM	Beta *	5.3
REM	High beta *	6
REM	Low gamma *	5.04
REM	High gamma	3.6

The ratio of mean power levels among SNc lensioned and control animals at a given frequency band is used to reflect the rise in synchronization in EEG. The increase in synchronization is observed in the SNc lesioned animals ($N = 9$, age = 8 w.o.) in comparison to the controls ($N = 9$, age = 8 w.o.) at each frequency band during wake, NREM, and REM. To assess statistical significance, a Welch's t-test was applied to the results at each frequency band with * denoting p-value < 0.05. Of all frequency bands, only high gamma for REM sleep and wake was not significant.

A high accuracy rate when using the ML pipeline to differentiate SNc lesioned animals from control animals during wake, REM, and NREM sleep indicated robust differences between the two groups (Fig. 2(**C**)). The ML pipeline also provided a high accuracy when considering all seven features at a single spectral band – namely, delta, alpha, beta, high beta, and low gamma EEG during wake, NREM sleep, and REM sleep (Fig. 2(**C**)). Using the statistical features of all EEG spectral bands resulted in an accuracy rate of approximately 0.65 in wake, NREM sleep, and REM sleep for differentiating SNc lesioned from controls. The accuracy rate attained when considering the deviation features across all EEG spectral bands was 0.748 during wake and 0.637 for REM sleep while only 0.519 for NREM sleep (Fig. 2(**D**)). Similar results were noted with the L1-LR technique although the predictive capability was degraded in the high beta band and not the high gamma band. Also, when using L1-LR, the predictive capability was rather poor during REM sleep when considering all features or only the deviation features (Fig. 2(**C**,**D**)). Lastly, the ML pipeline applied to all features form the single frequency of 40 Hz provided a differentiation of SNc lesioned animals from the controls. Despite several of the features being close to but not statistically significant (Fig. 3(**A**)), the collective 40 Hz features at wake, NREM, and REM sleep all yielded accuracy rates greater than 0.65 (Fig. 3(**B**)). Similar results were noted when using L1-LR in the ML pipeline with the exception of the predictive accuracy during REM sleep not exceeding 0.65 (AR = 0.636).

In summary, SNc lesions (nigrostriatal dopamine depletion) increased EEG synchronization across spectra (0.5–60 Hz) during wake, NREM sleep, and REM sleep. A ML technique trained on EEG features computed from a single or multiple spectral bands was able to differentiate SNc lesioned animals from controls at high accuracy during wake, NREM sleep, or REM sleep.

DISCUSSION

The basal ganglia regulates cortical activity and functions via its reciprocal topographical connectivity with the cerebral cortex. Nigrostriatal dopamine serves as a critical input to the basal ganglia by tuning cortical activity. Animal studies have established the neural circuitry underlying nigrostriatal dopamine control of cortical activity (Cooper and Stanford, 2001; Vetrivelan et al., 2010; Chen et al., 2015; Qiu et al., 2019) with

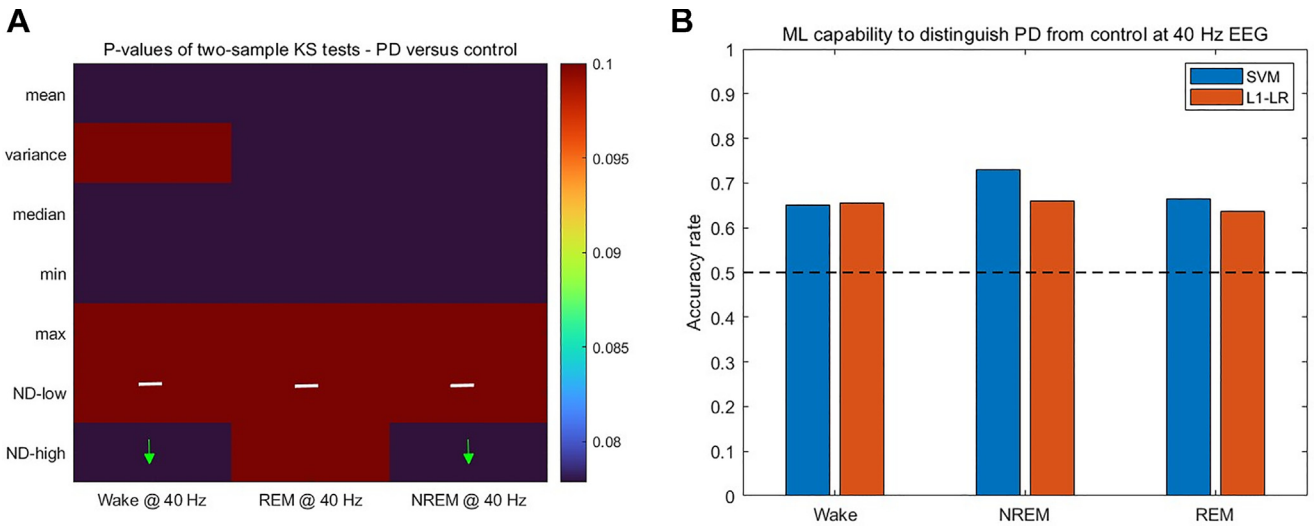

Fig. 3. Differentiations of 40 Hz EEG in sleep-wake states between SNc lesioned and control rats. The Kolmogorov-Smirnov tests indicate that during the three sleep-wake states two-thirds (i.e. 14/21) of the EEG features between the control (N = 9, age = 8 w.o.) and lesioned groups (N = 9, age = 8 w.o.) are close to statistical significance. The green arrows denote features that showed a decrease in value for SNc lesioned rats compared to controls while the white bars denote a feature that did not change in value among the two conditions (**A**). The ML pipeline with an SVM applied to the 40 Hz EEG features during wake, NREM sleep, and REM sleep resulted in accuracy rates greater than 0.65 for differentiating SNc lesioned animals from controls. Similar results were noted when using L1-LR in the ML pipeline except for the predictive accuracy during REM sleep not exceeding 0.65 (AR = 0.636). The black, dashed line indicates the chance predictive value of 0.5 for binary classification (**B**).

nigrostriatal dopamine acting on dopamine D2 inhibitory auto-receptors at the presynaptic sites of GABAergic striatiopallidal axons to elevate the firing of GABAergic pallidocortical neurons that inhibit the cortex (Chen et al., 2015). Thus, removal of nigrostriatal dopaminergic inputs to the basal ganglia in PD or by SNc lesions in rodents is hypothesized to increase cortical activity and arousal. Consistent with this notion, we have shown that SNc lesions increased total wake amounts and cortical c-Fos expression in rats (Qiu et al., 2014, 2016b). Conversely, we have shown that chemogenetic stimulation of SNc dopaminergic neurons promote sleep (Qiu et al., 2016b, 2019), and deep brain stimulation (DBS) in the GPe promotes sleep in rats (Qiu et al., 2016a). In the current study, we demonstrated that SNc lesions increased EEG power across 0.5–60 Hz during wake, NREM sleep, and REM sleep. We have defined the ratio of mean EEG power across a frequency band between lesioned and control animals as an indicator of a rise in the synchronization level. The elevated EEG power and the observed rise in synchronization is believed to be caused by elevated firing in cortical neurons as single-unit recordings have shown increased firing in cortical neurons following SNc lesions in primates (Wang et al., 2018).

The SNc lesions increased EEG synchronization unevenly across the EEG spectral bands in wake, REM, and NREM sleep. The wake beta, REM sleep high gamma, theta during wake and REM sleep, alpha in wake and NREM sleep, and delta, high beta, and low gamma in all three states showed such an effect. The sleep-wake-state dependent EEG synchronization after the SNc lesions indicates SNc dopamine control of the basal ganglia and cortical activity in sleep-wake state. Volition movement is believed to be regulated by a sequence of neuronal activity consisting of 0.5 s pre-onset reduction and onset activation shown in beta EEG in the premotor cortex (Satow et al., 2004) which is significantly altered by PD (Georgiev et al., 2016). The application of DBS in the subthalamic nucleus (STN) which reciprocally connects the GPe has been shown to correct abnormal beta EEG and motor symptoms in PD (Anidi et al., 2018). This suggests that extremely high beta EEG in the motor cortex during PD causes abnormal movements. Studies on EEG changes in human and animal PD models have primarily focused on movement related beta activity during wake state (West et al., 2018; Deffains and Bergman, 2019), although elevated beta activity is also found in NREM sleep in primate PD (Mizrahi-Kliger et al., 2020). The presented results further detailed sub-beta EEG changes. More, specifically, the beta (12.5–20 Hz) features were significantly different during wake while the high beta (20.5–30 Hz) features were significantly different in all three states (Fig. 2 and Table 1). Overall, increased EEG synchronization by SNc lesions is in line with reduction in EEG complexity in human PD (Yi et al., 2017; Keller et al., 2020). Although our analysis did not extend beyond 60 Hz it is conceivable that elevated synchronization may occur in EEG signals greater than 60 Hz since EEG changes by selective SNc lesions in rats are consistent with human EEG changes in PD. This also supports an assertion that EEG changes in PD are due to SNc lesions. We remark that the designations low gamma (30.5–40 Hz) and high gamma (40.5–60 Hz) are somewhat relative, i.e. they have been selected from existing literature (Cavelli et al., 2015; Milikovsky et al., 2017).

The deviation features in the EEG spectra were less altered by SNc lesions than the statistical features. An exception was the ND-high feature at high gamma EEG in REM sleep. Since the statistical features in high

gamma EEG during REM sleep were not significantly increased, the alteration in the deviation features points towards the role of dopamine at inducing high gamma oscillations during REM sleep. High gamma oscillation is generated by the hippocampus during REM sleep (Buzsaki et al., 2003) while SNc dopamine neurons discharge in a bursting pattern that may increase dopamine release in bursting mode during REM (Dahan et al., 2007). The loss of SNc dopamine may increase high gamma EEG spike amplitudes, resulting in increased ND-high values. Due to the absence of direct anatomical connections between the basal ganglia and the hippocampus, SNc dopamine may control the hippocampus via the entorhinal cortex that closely communicates with the hippocampus. As the entorhino-hippocampal complex generated theta and high gamma oscillations process emotional memory during REM sleep (Murkar and De Koninck, 2018), high theta and gamma EEG power by entorhinal cortex and the hippocampus (Chrobak and Buzsaki, 1998) may contribute to cognitive and mental declines in PD (Weintraub and Mamikonyan, 2019; Zhu et al., 2019) as well as the vivid dreaming in PD (Otaiku, 2021).

The topographic connections of the basal ganglia and the cortex are consistent with the increased synchronization across global EEG spectra in sleep-wake states following the removal of nigrostriatal dopamine inputs to the basal ganglia. The presented ML analysis on the EEG features computed across all spectral bands during wake, NREM, and REM identified SNc lesions with high accuracy. Furthermore, the ML pipeline with features computed at the single frequency of 40 Hz in sleep-wake state identified SNc lesions at high accuracy. Although beta EEG power increase has been studied as a biomarker of PD (Bore et al., 2020), studies have shown that beta EEG alone is not a sufficient biomarker (Connolly et al., 2015; Zhang et al., 2021). Our findings suggest that multiple EEG bands exhibit a larger and more patent difference than a single frequency band in PD. The onset of the motor symptoms associated with PD typically start when there is substantial SNc neuronal loss totaling 70–80% (Savica et al., 2010). Thus, it is likely that EEG changes start in the pre-motor stage and worsen in the motor stage of PD. It has been established that REM sleep behavior disorder (RBD) is a biomarker of pre-motor PD (Schenck et al., 2003; Barone and Henchcliffe, 2018). However, there are substantial (i.e. 20–70%) cases of RBD without PD, as well as an estimated 75% of PD cases that are not accompanied with RBD (Zhang et al., 2017a; 2017b). Nevertheless, PD-like traits in EEG signals during wake and sleep have been reported in people with RBD (Hackius et al., 2016). We believe that PD-like traits shown in EEG recordings would predict pre-motor PD more accurately than RBD. This is in light of considering that RBD is an indicator of synucleinopathies including PD, multiple system atrophy (MSA), and dementia with Lewy bodies while the rise in EEG synchronization during sleep-wake states is unique to the SNc lesions. This is consistent with high beta power reported in EEG recordings in Wilson's disease (Dierks et al., 1999; Tamas et al., 2011). Our analyses suggest that PD-like EEG features may detect other basal ganglia disorders such as Wilson's disease (copper accumulation in the basal ganglia) and Farh's Disease (calcification in the basal ganglia). A future avenue will encompass exploiting neural signals by using ML to identify other EEG features as well as considering greater than 60 Hz frequencies in SNc lesioned animals. The results are indicative of EEG being a powerful biomarker for other basal ganglia and cortical dysfunctions such as Huntington's disease and dementia.

FUNDING

The authors acknowledge funding from the Science and technology department of Jilin province (20180623052TC) and Jilin provincial key laboratory (20190901005JC).

REFERENCES

Anidi C, O'Day JJ, Anderson RW, Afzal MF, Syrkin-Nikolau J, Velisar A, Bronte-Stewart HM (2018) Neuromodulation targets pathological not physiological beta bursts during gait in Parkinson's disease. Neurobiol Dis 120:107–117.

Barone DA, Henchcliffe C (2018) Rapid eye movement sleep behavior disorder and the link to alpha-synucleinopathies. Clin Neurophysiol 129:1551–1564.

Bore JC, Campbell BA, Cho H, Gopalakrishnan R, Machado AG, Baker KB (2020) Prediction of mild parkinsonism revealed by neural oscillatory changes and machine learning. J Neurophysiol 124:1698–1705.

Buzsaki G, Buhl DL, Harris KD, Csicsvari J, Czeh B, Morozov A (2003) Hippocampal network patterns of activity in the mouse. Neuroscience 116:201–211.

Buzsaki G, Draguhn A (2004) Neuronal oscillations in cortical networks. Science 304:1926–1929.

Cavelli M, Castro S, Schwarzkopf N, Chase MH, Falconi A, Torterolo P (2015) Coherent neocortical gamma oscillations decrease during REM sleep in the rat. Behav Brain Res 281:318–325.

Chen MC, Ferrari L, Sacchet MD, Foland-Ross LC, Qiu MH, Gotlib IH, Fuller PM, Arrigoni E, Lu J (2015) Identification of a direct GABAergic pallidocortical pathway in rodents. Eur J Neurosci 41:748–759.

Chrobak JJ, Buzsaki G (1998) Operational dynamics in the hippocampal-entorhinal axis. Neurosci Biobehav Rev 22:303–310.

Connolly AT, Jensen AL, Baker KB, Vitek JL, Johnson MD (2015) Classification of pallidal oscillations with increasing parkinsonian severity. J Neurophysiol 114:209–218.

Cooper AJ, Stanford IM (2001) Dopamine D2 receptor mediated presynaptic inhibition of striatopallidal GABA(A) IPSCs in vitro. Neuropharmacology 41:62–71.

Dahan L, Astier B, Vautrelle N, Urbain N, Kocsis B, Chouvet G (2007) Prominent burst firing of dopaminergic neurons in the ventral tegmental area during paradoxical sleep. Neuropsychopharmacology 32:1232–1241.

Deffains M, Bergman H (2019) Parkinsonism-related beta oscillations in the primate basal ganglia networks - Recent advances and clinical implications. Parkinsonism Relat Disord 59:2–8.

Dierks T, Kuhn W, Oberle S, Muller T, Maurer K (1999) Generators of brain electrical activity in patients with Wilson's disease. Eur Arch Psychiatry Clin Neurosci 249:15–20.

Georgiev D, Lange F, Seer C, Kopp B, Jahanshahi M (2016) Movement-related potentials in Parkinson's disease. Clin Neurophysiol 127:2509–2519.

Guo CN, Yang WJ, Zhan SQ, Yang XF, Chen MC, Fuller PM, Lu J (2017) Targeted disruption of supraspinal motor circuitry reveals a

distributed network underlying Restless Legs Syndrome (RLS)-like movements in the rat. Sci Rep 7:9905.
Hackius M, Werth E, Surucu O, Baumann CR, Imbach LL (2016) Electrophysiological Evidence for Alternative Motor Networks in REM Sleep Behavior Disorder. J Neurosci 36:11795–11800.
Keller SM, Gschwandtner U, Meyer A, Chaturvedi M, Roth V, Fuhr P (2020) Cognitive decline in Parkinson's disease is associated with reduced complexity of EEG at baseline. Brain Commun 2: fcaa207.
Milikovsky DZ, Weissberg I, Kamintsky L, Lippmann K, Schefenbauer O, Frigerio F, Rizzi M, Sheintuch L, Zelig D, Ofer J, Vezzani A, Friedman A (2017) Electrocorticographic Dynamics as a Novel Biomarker in Five Models of Epileptogenesis. J Neurosci 37:4450–4461.
Mizrahi-Kliger AD, Kaplan A, Israel Z, Deffains M, Bergman H (2020) Basal ganglia beta oscillations during sleep underlie Parkinsonian insomnia. Proc Natl Acad Sci U S A 117:17359–17368.
Murkar ALA, De Koninck J (2018) Consolidative mechanisms of emotional processing in REM sleep and PTSD. Sleep Med Rev 41:173–184.
Otaiku AI (2021) Dream Content Predicts Motor and Cognitive Decline in Parkinson's Disease. Mov Disord Clin Pract 8:1041–1051.
Qiu MH, Chen MC, Huang ZL, Lu J (2014) Neuronal activity (c-Fos) delineating interactions of the cerebral cortex and basal ganglia. Front Neuroanat 8:13.
Qiu MH, Chen MC, Wu J, Nelson D, Lu J (2016a) Deep brain stimulation in the globus pallidus externa promotes sleep. Neuroscience 322:115–120.
Qiu MH, Yao QL, Vetrivelan R, Chen MC, Lu J (2016b) Nigrostriatal Dopamine Acting on Globus Pallidus Regulates Sleep. Cereb Cortex 26:1430–1439.
Qiu MH, Zhong ZG, Chen MC, Lu J (2019) Nigrostriatal and mesolimbic control of sleep-wake behavior in rat. Brain Struct Funct 224:2525–2535.
Satow T, Ikeda A, Yamamoto J, Begum T, Thuy DH, Matsuhashi M, Mima T, Nagamine T, Baba K, Mihara T, Inoue Y, Miyamoto S, Hashimoto N, Shibasaki H (2004) Role of primary sensorimotor cortex and supplementary motor area in volitional swallowing: a movement-related cortical potential study. Am J Physiol Gastrointest Liver Physiol 287:G459–G470.
Savica R, Rocca WA, Ahlskog JE (2010) When does Parkinson disease start? Arch Neurol 67:798–801.
Schenck CH, Callies AL, Mahowald MW (2003) Increased percentage of slow-wave sleep in REM sleep behavior disorder (RBD): a reanalysis of previously published data from a controlled study of RBD reported in SLEEP. Sleep 26:1066. author reply 1067.
Sharott A, Magill PJ, Harnack D, Kupsch A, Meissner W, Brown P (2005) Dopamine depletion increases the power and coherence of beta-oscillations in the cerebral cortex and subthalamic nucleus of the awake rat. Eur J Neurosci 21:1413–1422.
Tamas G, Raethjen J, Muthuraman M, Folhoffer A, Deuschl G, Szalay F, Takats A, Kamondi A (2011) Disturbed post-movement beta synchronization in Wilson's disease with neurological manifestation. Neurosci Lett 494:240–244.
Vetrivelan R, Qiu MH, Chang C, Lu J (2010) Role of Basal Ganglia in sleep-wake regulation: neural circuitry and clinical significance. Front Neuroanat 4:145.
Wang M, Song Y, Zhang S, Xu S, Xiao G, Li Z, Gao F, Zhang Y, Yue F, Chan P, Cai X (2018) Abnormal Spontaneous Neuronal Discharge and Local Field Potential both in Cortex and Striatum of a Non- human Primate of Parkinson's Disease using Implantable Microelectrode Arrays. Annu Int Conf IEEE Eng Med Biol Soc 2018:1–4.
Weintraub D, Mamikonyan E (2019) The Neuropsychiatry of Parkinson Disease: A Perfect Storm. Am J Geriatr Psychiatry 27:998–1018.
West TO, Berthouze L, Halliday DM, Litvak V, Sharott A, Magill PJ, Farmer SF (2018) Propagation of beta/gamma rhythms in the cortico-basal ganglia circuits of the parkinsonian rat. J Neurophysiol 119:1608–1628.
Yi GS, Wang J, Deng B, Wei XL (2017) Complexity of resting-state EEG activity in the patients with early-stage Parkinson's disease. Cogn Neurodyn 11:147–160.
Zhang J, Xu CY, Liu J (2017a) Meta-analysis on the prevalence of REM sleep behavior disorder symptoms in Parkinson's disease. BMC Neurol 17:23.
Zhang J, Idaji MJ, Villringer A, Nikulin VV (2021) Neuronal biomarkers of Parkinson's disease are present in healthy aging. Neuroimage 243 118512.
Zhang X, Sun X, Wang J, Tang L, Xie A (2017b) Prevalence of rapid eye movement sleep behavior disorder (RBD) in Parkinson's disease: a meta and meta-regression analysis. Neurol Sci 38:163–170.
Zhu M, HajiHosseini A, Baumeister TR, Garg S, Appel-Cresswell S, McKeown MJ (2019) Altered EEG alpha and theta oscillations characterize apathy in Parkinson's disease during incentivized movement. Neuroimage Clin 23 101922.

(Received 5 August 2022, Accepted 28 November 2022)
(Available online 5 December 2022)